

Upper limit on a time reversal noninvariant part of Wigner's random matrix model*

H. S. Camarda

Lawrence Livermore Laboratory, University of California, Livermore, California 94550

(Received 24 November 1975)

The results of a Monte Carlo investigation and comparison with experimental data of Wigner's random matrix model with differing amounts of a time reversal noninvariant part are presented. With $H_{ij} = R_{ij} + iyI_{ij}$, calculations were performed with $y = 0.00, 0.05, 0.10, 0.20, 0.50,$ and 1.00 using 40×40 matrices and $y = 0.00, 0.05,$ and 0.10 with 80×80 matrices. After unfolding the density variation of the eigenvalues the behavior of the Dyson-Mehta Δ_3 statistic was examined for different values of y . The behavior of the reduced widths, which has also been examined in a previous calculation by Rosenzweig, Monahan, and Mehta, was found to be considerably more sensitive to small y values than the Δ_3 statistic. Thus the reduced width data can place a much lower limit on y than the level spacing information. A comparison of the calculations performed here with recently collected high quality neutron resonance data gives $y < 0.05$ at the 99.7% confidence level. It is also shown that the same value of the Dyson-Mehta Δ_3 statistic results when the matrix elements of Wigner's model are chosen from a Gaussian or flat distribution.

NUCLEAR STRUCTURE Monte Carlo calculation, Wigner's random matrix model. Effect of time reversal violation on statistical behavior of resonances. Comparison with experimental data.

INTRODUCTION

The statistical behavior of level spacings and reduced widths of compound nuclear states is well described, in the absence of intermediate structure effects, by Wigner's orthogonal ensemble (OE).¹ In this theory the Hamiltonian of a physical system is representative of an ensemble of real symmetric matrices which obey certain statistical laws. Real symmetric matrices were chosen in order to describe systems which are invariant under time reversal. Other ensembles of matrices can be defined^{1,2} which would be applicable to physical systems obeying different conservation laws; for example, an ensemble of Hermitian matrices [called the unitary ensemble (UE)] would represent systems without time reversal symmetry. The OE and UE predict significantly different behavior for level spacings and reduced widths.¹ When the physical system being described is so complicated that the detailed nature of the interactions is unimportant, the statistical behavior of the level spacings and reduced widths is sensitive to the laws of symmetry.

The main purpose of this paper is to determine what limit can be placed on a time reversal noninvariant part of Wigner's random matrix model from the high quality resonance data (mainly neutron data) collected only recently.³⁻¹⁶ Earlier calculations¹⁷ of this nature stressed the effect of a small violation of time reversal on the statistical behavior of the nearest neighbor spacing distribution and on the distribution of reduced widths, but no serious comparison with experimental data was

ever made. Here the emphasis is on the long range correlations between level spacings as well as on the reduced widths.

CALCULATION

The OE is defined by the set of $N \times N$ real symmetric matrices which have matrix elements that are statistically independent and obey Gaussian probability distributions, centered about zero, with the variance of the diagonal elements being twice that of the off diagonal elements.¹ The eigenvalues of these matrices are distributed according to the Wishart distribution¹⁸:

$$P(E_1, \dots, E_N) dE_1 \cdots dE_N \sim \prod_{i < j} |E_i - E_j|^\beta \exp\left(-\sum_i E_i^2 / 4\sigma^2\right) dE_1 \cdots dE_N. \quad (1)$$

$\beta = 1$, σ^2 is the variance of the nondiagonal matrix elements, and N is the matrix dimension. This eigenvalue distribution describes the behavior of a single population (levels of a given nucleus characterized by the same spin and parity) of resonance energies which are observed experimentally. The eigenvalue density is symmetric about zero and in the limit of large matrix dimensions is described by Wigner's semicircular law¹⁹:

$$P_w(g) dg = \frac{1}{\pi} [1 - (\frac{1}{2}g)^2]^{1/2} dg, \quad g = E/\sigma(\beta N)^{1/2}. \quad (2)$$

For the OE $\beta = 1$. Since the experimental data are

characterized by a constant level density (an exception is the proton data discussed below), either very large matrices must be diagonalized and only the central portion of constant density used, or a transformation from the semicircular distribution to a constant density must be made. For all the calculations performed here the latter approach was used since it was found to be a correct procedure in a previous calculation.^{3,6}

Wigner's model also describes the behavior of the reduced widths of the resonances. Borrowing the definition of the reduced width from R matrix theory,²⁰ one has

$$\Gamma_{\lambda c} \sim \gamma_{\lambda c}^2, \quad \gamma_{\lambda c} \sim \int X_{\lambda} \phi_c dS, \quad (3)$$

where $\gamma_{\lambda c}$ is real, ϕ_c is a channel wave function, and X_{λ} is one of a complete set of states defined in the interaction region; the integration is carried out in a $3(A-1)$ dimensional space (A is the number of nucleons of the compound system). Associating X_{λ} with the eigenstates of the random matrices and expressing X_{λ} in terms of its components $a_{j\lambda}$ with respect to the original basis ψ_j gives

$$\gamma_{\lambda c} = \sum_j a_{j\lambda} S_{jc}, \quad S_{jc} = \int \psi_j \phi_c dS. \quad (4)$$

Porter and Rosenzweig²¹ showed that the $a_{j\lambda}$'s obey Gaussian distributions, centered about zero, and applied the central limit theorem to the sum. This implies a Gaussian distribution for the $\gamma_{\lambda c}$'s and consequently the Porter-Thomas²² (PT) distribution for the reduced widths. In the calculations performed here S_{jc} is taken to be constant.

The extension to the time reversal noninvariant case can be made by letting each matrix element become complex, i.e.,

$$H_{ij} = R_{ij} + i y I_{ij}, \quad (5)$$

where hermiticity requires $R_{ij} = R_{ji}$ and $I_{ij} = -I_{ji}$. y is a measure of the strength of the part violating time reversal. R_{ij} and I_{ij} are statistically independent and the I_{ij} 's obey Gaussian probability distributions with the same variance as the R_{ij} 's ($i \neq j$). The reduced widths are proportional to $\gamma_{\lambda c} \gamma_{\lambda c}^*$ ($\gamma_{\lambda c}$ is now complex), and S_{jc} was again chosen to be constant. When $y = 1.0$ this becomes the UE and Eqs. (1) and (2) apply with $\beta = 2.0$.¹

With the model above, Monte Carlo calculations were performed wherein sets of 40×40 and 80×80 matrices were diagonalized as summarized in Table I. For the cases $y = 0.0$ and 1.0 analytical solutions are known, and these serve as a check on the calculations. For example, Fig. 1(a) shows the eigenvalue distribution of the 40×40 matrices for the cases $y = 0.0, 0.5,$ and 1.0 . For $y = 0.0$ and 1.0 , the semicircular law is applicable with $\beta = 1$ and 2 ,

TABLE I. Summary of the number of matrices of a given dimension which were diagonalized. Y is a measure of the strength of a time reversal violating part of Wigner's random matrix model.

Matrix dimension	Number of matrices diagonalized	y
80	80	0.00
80	80	0.05
80	150	0.10
40	150	0.00
40	150	0.05
40	150	0.10
40	70	0.20
40	70	0.50
40	70	1.00
40 ^a	150	0.00
80 ^a	60	0.10

^a Matrix elements chosen from a flat distribution centered about zero.

respectively. As can be seen, the agreement is good except at the extreme ends where deviations due to the finite matrix size are expected. For values of y intermediate between 0.0 and 1.0 the eigenvalue distribution is believed to follow the semicircular law. Figure 1(a) indicates that, to within statistics, the semicircular law with $\beta = 1.22$ gives a good fit when $y = 0.5$. Furthermore, it was found that for $y \leq 0.1$, the semicircular law with $\beta = 1.0$ fitted the Monte Carlo results well. This is demonstrated in Fig. 1(b) for the 80×80 matrices.

For the OE ($y = 0.0$) the reduced widths for a single channel are predicted¹ to follow the PT distribution:

$$P(x) dx = (2/\pi)^{1/2} e^{-x^2/2} dx, \quad x = (\gamma_c^2 / \langle \gamma_c^2 \rangle)^{1/2}, \quad (6)$$

while for the UE ($y = 1.0$), the expected distribution¹ of widths is

$$P(x) dx = 2x e^{-x^2} dx. \quad (7)$$

The variances ($V = \langle x^2 \rangle - 1$) for these distributions are 2.0 and 1.0, respectively. In Fig. 2 the quantity V is plotted as a function of y for the 40×40 and 80×80 matrix generated widths (the error bars reflect the uncertainty due to the finite sample size). The values of V found here²³ are in good agreement with those of Rosenzweig *et al.*¹⁷ and confirm their conclusion about its sensitivity to small values of y . These authors also demonstrated that the value of V is dependent on the matrix dimension. This is implied by the $y = 0.1$ results of Fig. 2 where the value of V determined from the widths generated by diagonalizing the 80×80 matrices lies below that calculated with the 40×40 matrices.

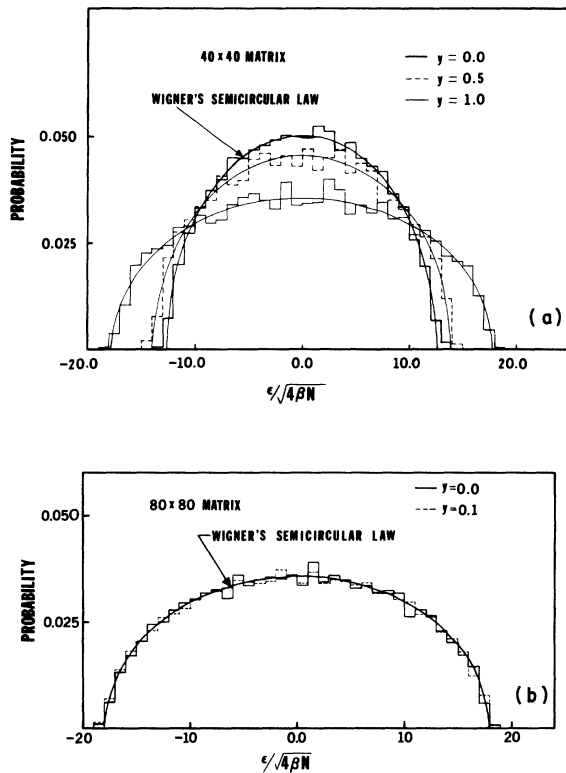


FIG. 1. The eigenvalue distribution generated by diagonalizing (a) 40×40 matrices with the strength of the time reversal violating part $y=0.0, 0.5$, and 1.0 and similarly for the (b) 80×80 matrices with $y=0.0$ and 0.1 . The smooth curves represent Wigner's semicircular law.

A sensitive test of the long range correlations between level spacings is the Dyson-Mehta Δ_3 statistic.²⁴ This statistic is a measure of the mean square deviation of a staircase plot of a sequence of n levels from a best fitting straight line; i.e.,

$$\Delta_3 = \text{Min}_{A,B} \frac{1}{\Delta E} \int_0^{\Delta E} [N(E) - AE - B]^2 dE. \quad (8)$$

$N(E)$ is the number of levels between zero and energy E [a graph of $N(E)$ vs E resembles a staircase]. Using Dyson's circular orthogonal ensemble theory²⁵ (this is equivalent to Wigner's OE) where the eigenvalues have a constant density, Dyson and Mehta²⁴ calculated the expected behavior of Δ_3 and its standard deviation (SD). For a single population of levels they found

$$\langle \Delta_3 \rangle = \frac{1}{\pi^2} [\ln n - 0.0687], \quad (9)$$

$$\text{SD of } \Delta_3 = 0.11.$$

The logarithmic dependence of $\langle \Delta_3 \rangle$ on the number

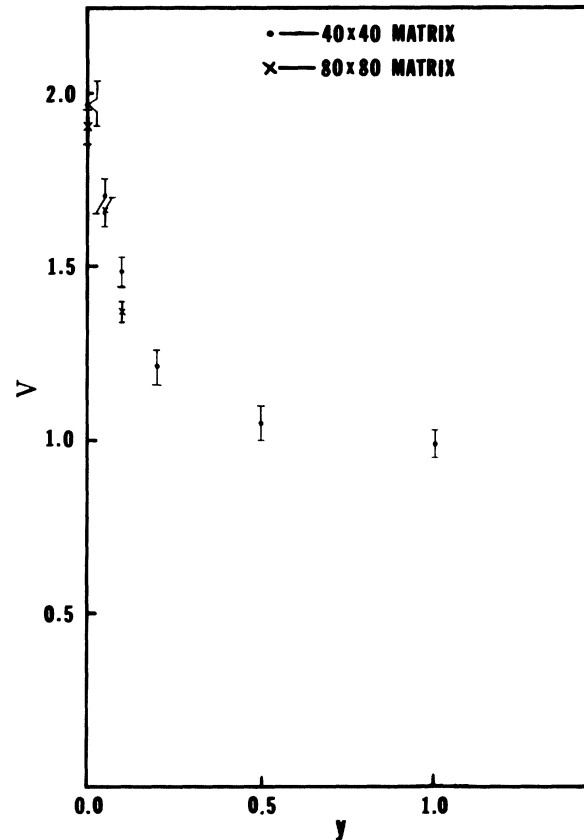


FIG. 2. Plot of the variance ($V = \langle x^2 \rangle - 1$) of the Monte Carlo generated reduced widths for the 40×40 and 80×80 matrices as a function of y . The errors are due to the finite sample size.

of levels reflects the long range correlations between level spacings. For level spacings which are uncorrelated the average value of Δ_3 has a linear dependence on n ($n \gg 1$).^{3,6} In evaluating Δ_3 from the Monte Carlo generated sets of eigenvalues, the following procedure was used. First, two eigenvalues from each end of the eigenvalue distribution were discarded and the transformation $P_w(g) dg = P(u) du$ was made with $P(u)$ set equal to a constant. $P_w(g)$ is the semicircular law with an appropriate value of N and β . The resulting sets of constant density eigenvalues were then used to evaluate the Δ_3 statistic. Table II lists the values of $\bar{\Delta}_3$ and SD of Δ_3 determined from the 40×40 and 80×80 matrices for $y=0.0$ and 0.1 along with the values predicted by Eq. (9). The agreement of the $y=0.0$ results with Eq. (9) is good.

Some time ago Rosenzweig²⁶ demonstrated, through Monte Carlo calculations, that OE matrices with matrix elements obeying flat (instead of Gaussian) distributions centered about zero resulted in a nearest neighbor spacing distribution

TABLE II. Behavior of the Δ_3 statistic and SD of Δ_3 from the Monte Carlo generated eigenvalues for $y=0.0$ and 0.1 and for matrix elements chosen from flat and Gaussian distributions. The OE predictions are also given.

Matrix dimension	y	Eigenvalues used	$\bar{\Delta}_3$	SD of Δ_3	$\langle \Delta_3 \rangle$	SD of Δ_3
40	0.0	36	0.359 ± 0.008	0.09	0.356	0.11
80	0.0	76	0.423 ± 0.012	0.11	0.432	0.11
40 ^a	0.0	36	0.371 ± 0.009	0.11	0.356	0.11
80	0.10	76	0.377 ± 0.009	0.11		
80 ^a	0.10	76	0.380 ± 0.012	0.09		

^a Matrix elements chosen from a flat distribution centered about zero.

in good agreement with the OE spacing law suggested by Wigner. (Wigner's law has a simple analytical form and differs little from the exact OE nearest neighbor spacing distribution found by Gaudin²⁷; the difference cannot be distinguished experimentally.) It is not known how matrix elements drawn from a flat distribution would affect the long range correlations between level spacings. Results of a calculation performed here with matrix elements obeying a flat distribution for the case $y=0.0$ are presented in the third row of Table II. As can be seen, no significant difference between the values of $\bar{\Delta}_3$ and SD of Δ_3 for the Gaussian and flat matrix element distribution is evident. It is worth noting that the flat distribution, like the Gaussian distribution, leads to a joint probability distribution for the matrix elements which is invariant under a change of basis vectors.

Plotted in Fig. 3 is $\bar{\Delta}_3$ as a function of y calculated for 36 levels using both the 40×40 and 80×80 matrix results. The point at $y=0.0$ was calculated using Eq. (9). In comparing Fig. 3 with Fig. 2 it is clear that $\bar{\Delta}_3$ does not decrease as rapidly as V for small values of y . Therefore, the behavior of the reduced widths will be a more sensitive test for setting an upper limit on the value of y . The values of $\bar{\Delta}_3$ plotted in Fig. 3 for $y=0.1$ indicate a dependence on the matrix dimension similar to that observed for V . As a result only the 80×80 matrix results were used for comparison with the experimental data. Figure 4 shows $\bar{\Delta}_3$ as a function of n , the number of levels, for $y=0.00, 0.05,$ and 0.10 . [The $y=0.00$ curve was generated using Eq. (9).] In order to increase the statistical accuracy of $\bar{\Delta}_3$ evaluated for $n=14$ and 36 , different sections of the 80×80 eigenvalue sets were used. It was found that for $n=36$ good agreement for $\bar{\Delta}_3$ was obtained using eigenvalues 3–38, 22–57, or 40–75. Similar results were found for the $n=14$ case, indicating that the transformation of the eigenvalues to a constant density, as described above, is a valid procedure.

In the last two rows of Table II are given $\bar{\Delta}_3$ and SD of Δ_3 found for the 80×80 matrices with $y=0.1$ when the matrix elements are chosen from Gaussian and flat distributions. Again, as for the $y=0.0$ case, there is no significant difference between the two results.

COMPARISON WITH EXPERIMENT

A sequence of levels characterized by the same spin and parity (a single population of levels) rep-

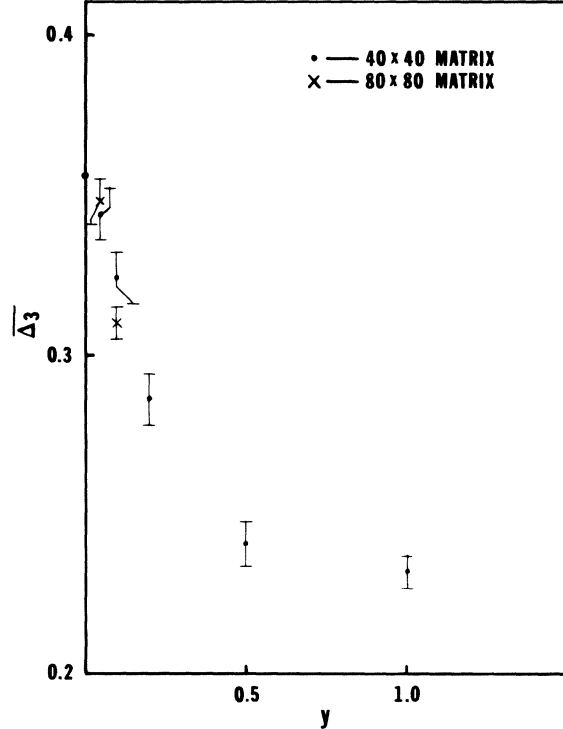


FIG. 3. The average value of the Dyson-Mehta Δ_3 statistic evaluated (after unfolding the density variation of the eigenvalues) for 36 levels from the 40×40 and 80×80 matrix results for different values of y . The point at $y=0.0$ was determined from Eq. (9).

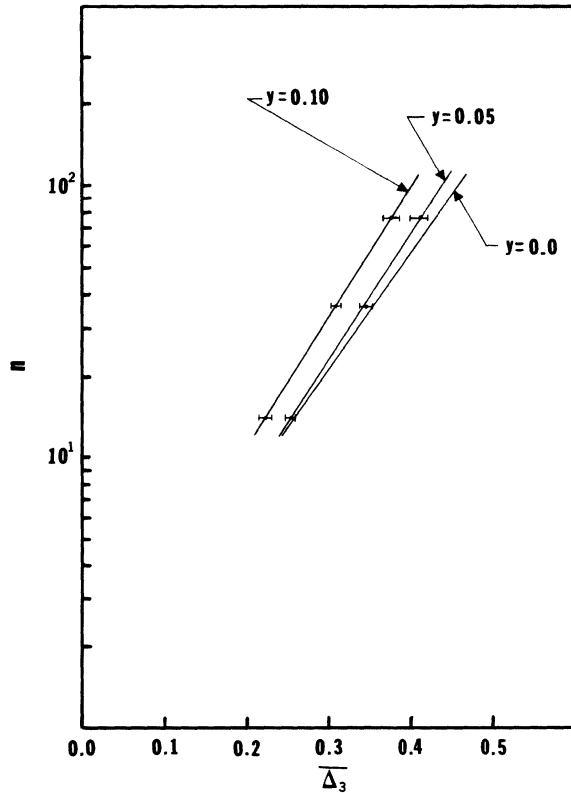


FIG. 4. The behavior of $\bar{\Delta}_3$ for $\gamma=0.00, 0.05,$ and 0.10 as a function of n , the number of levels. The uncertainty of $\bar{\Delta}_3$ for $\gamma=0.05$ and 0.10 results from the finite number of sets of eigenvalues. Equation (9) was used to determine the $\gamma=0.0$ curve.

resents the best data for placing a limit on a time reversal noninvariant part of Wigner's random matrix model. For neutron data the most satisfactory target nuclei are the even-even isotopes in the rare earth region of the periodic table. These nuclei have zero spin and always form $J = \frac{1}{2}$, even parity states with s -wave neutrons. For the rare earth nuclei the ratio of the p -wave to s -wave strength function is generally less than one, leading to a cleaner separation between small s levels and large p levels, i.e., there will be a better chance of detecting all the weak $l=0$ levels without detecting any p levels. Furthermore, these nuclei contain a statistically significant number of levels in the energy range where current experimental resolution is capable of detecting "all" the s -wave resonances. $l=0$ neutrons incident upon odd A target nuclei ($I \neq 0$) will form resonances with $J = I + \frac{1}{2}, I - \frac{1}{2}$ giving a sequence of levels which is a random mixture of two single populations. The spacing distribution of a two-spin population contains less information, and the absence of the "Wigner repul-

sion" between levels with different spin increases the probability of missing small $l=0$ levels. Thus the distribution of the reduced widths of the two-spin population will tend to be less reliable than the single population case. All the neutron data^{4-10,12-16} examined here was taken on target nuclei in the rare earth region of the Periodic Table. The incident neutron energy varied typically from zero to several keV. Consequently, the level densities and average reduced widths are, to a good approximation, constant.

In addition to neutron data, proton data of Wilson, Bilpuch, and Mitchel¹¹ were also used. The reduced width information of the proton data was not utilized because the measurements were carried out in the region of analog resonances, which causes the average reduced width to change rapidly. The incident proton energy spanned the range 1.5 to 3.0 MeV and, as a result, the data reflected the increase in level density with increasing excitation energy. In order to make a comparison with OE theory Wilson *et al.*¹¹ unfolded the level density variation using a procedure exactly paralleling that used above for the eigenvalues of the random matrices.

Table III lists the experimental values of Δ_3 found for different target nuclei along with the average value $\langle \Delta_3 \rangle$ predicted by OE theory for a single population of levels. For the Hf data the resonance spins were determined experimentally and single populations constructed.¹⁰ For the proton data, given in the last three rows of Table III, the spins and parities of the resonances were also determined experimentally.¹¹

In order to compare the Monte Carlo results with this experimental data the following statistic is used:

$$\Delta = \sum_J \Delta_3^J; \quad \sigma_\Delta^2 = \sum_J (\sigma_{\Delta_3^J})^2. \quad (10)$$

The sum is over the number of sets of levels and each Δ_3^J is evaluated for the appropriate number of levels. The experimental value of Δ for the 16 elements in Table III is 5.78, while the average values of Δ for the cases $\gamma=0.0$ and 0.1 (determined using the $\gamma=0.1$ curve of Fig. 4) are 5.79 and 5.04, respectively. For $\gamma \leq 0.1$ the behavior of Δ is well described by a Gaussian distribution with $\sigma_\Delta = 0.44$, and the probability of finding $\Delta \geq \Delta_{\text{exp}}$ is easily calculated and found to be, respectively, 0.50 and 0.05. The agreement with the OE is excellent, while the disagreement with the $\gamma=0.1$ case is significant enough to claim $\gamma \leq 0.1$.

Neutron widths are available only for the target nuclei in the first eight rows of Table III, i.e., ¹⁵²Sm through ¹⁸⁴W. It is desirable to combine the reduced width information of these eight nuclei in-

TABLE III. Tabulated values of Δ_3 found experimentally for single populations of levels along with the OE predictions. The neutron data is given in the first 13 rows.

Target nucleus	J^π of levels	Number of levels	Δ_3^{EXP}	$\langle \Delta_3 \rangle$	Ref.
^{152}Sm	$\frac{1}{2}^+$	70	0.41	0.42	4
^{154}Sm	$\frac{1}{2}^+$	27	0.38	0.32	4
^{154}Gd	$\frac{1}{2}^+$	19	0.22	0.28	5
^{158}Gd	$\frac{1}{2}^+$	47	0.29	0.38	5
^{166}Er	$\frac{1}{2}^+$	109	0.46	0.47	6
^{172}Yb	$\frac{1}{2}^+$	55	0.41	0.40	7
^{182}W	$\frac{1}{2}^+$	41	0.26	0.37	8
^{184}W	$\frac{1}{2}^+$	30	0.47	0.34	8
^{156}Gd	$\frac{1}{2}^+$	55	0.30	0.40	9
^{177}Hf	3^-	20	0.32	0.30	10
^{177}Hf	4^-	23	0.34	0.31	10
^{179}Hf	4^+	25	0.30	0.32	10
^{179}Hf	5^+	22	0.39	0.31	10
$^{44}\text{Ca}^a$	$\frac{1}{2}^+$	39	0.34	0.36	11
$^{44}\text{Ca}^a$	$\frac{1}{2}^-$	52	0.39	0.39	11
$^{48}\text{Ti}^a$	$\frac{1}{2}^+$	66	0.51	0.42	11

^a Proton data.

to a single histogram in order to obtain increased statistical precision. This was done in the following way: The 70 reduced neutron widths, Γ_n^0 's, of ^{152}Sm determined the average width $\langle \Gamma_n^0 \rangle = (1/N) \sum_J \Gamma_n^0$ associated with ^{152}Sm ($N=70$). Then a set of 70 normalized widths $\chi_J = \Gamma_n^0 / \langle \Gamma_n^0 \rangle$ was constructed for ^{152}Sm . The same procedure was used for the 27 levels of ^{154}Sm , etc. Since the statistical behavior of each set of χ_J 's is expected to be the same (i.e., the same first moment, second moment, etc.), the χ_J values for all the nuclei (^{152}Sm – ^{184}W) were combined into a single histogram. These experimental data consisting of a total of 398 normalized widths are represented by the solid histogram of Fig. 5.

The distribution of normalized widths when a 5% time reversal violating part was introduced into the random matrix model was obtained as follows: for each 80×80 matrix diagonalized (with $\gamma=0.05$) a set of 80 normalized reduced $\chi_{\lambda c} = |\gamma_{\lambda c}|^2 / \langle |\gamma_c|^2 \rangle$ ($\langle |\gamma_c|^2 \rangle = (1/N) \sum_\lambda |\gamma_{\lambda c}|^2$, $N=80$) was determined.²⁸ Then the 80 sets of $\chi_{\lambda c}$'s (total number of widths = 6400) were combined into a single histogram from which probabilities for finding $\chi_{\lambda c}$ between $\chi_{\lambda c}$ and $\chi_{\lambda c} + \Delta \chi_{\lambda c}$ could be calculated. In this manner the dashed histogram of Fig. 5 giving the expected behavior for 398 widths was found. The smooth curve of Fig. 5 is the Porter-Thomas distribution. As a measure of how well the dashed histogram and the

Porter-Thomas distribution of Fig. 5 fitted the experimental data, a χ^2 (chi-square) test was made. $\chi^2_{\text{EXP}} = \sum_i (e_i - o_i)^2 / e_i$, where e_i and o_i are the expected (dashed histogram or PT curve) and observed (solid histogram) number of "counts" in a histogram interval. The sum was carried out over the first seven histogram intervals. It was found

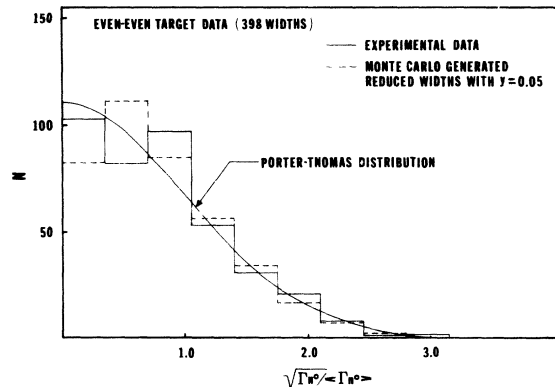


FIG. 5. The solid histogram gives the distribution of the combined normalized reduced neutron widths of the even-even target nuclei $^{152,154}\text{Sm}$, $^{154,158}\text{Gd}$, ^{166}Er , ^{172}Yb , and $^{182,184}\text{W}$. The dashed histogram is the expected reduced width distribution if a 5% time reversal violating part is introduced into Wigner's random matrix model. The smooth curve is the Porter-Thomas distribution.

TABLE IV. Values of Δ_3 found experimentally from two population neutron data. The OE predicted Δ_3 values for two randomly mixed single populations are given.

Target nucleus	Number of levels	Δ_3^{EXP}	$\langle \Delta_3 \rangle$	Ref.
^{151}Sm	64	0.54	0.69	12
^{163}Dy	30	0.50	0.53	13
^{167}Er	30	0.29	0.53	6
^{175}Lu	53	0.48	0.65	14
^{177}Hf	42	0.39	0.60	15
^{197}Au	112	0.78	0.79	16

that the probability P for finding $\chi^2 \leq \chi^2_{\text{EXP}}$ was 0.997 and 0.90, respectively, when the dashed histogram or the PT curve represented the expected neutron width distribution. The statistical behavior of the experimental data indicates any time reversal violating part of the random matrix model is $<5\%$. The value of P for the PT distribution is on the high side but still within acceptable limits.

Table IV lists odd A target nuclei for which $\Delta_3^{\text{EXP}} \leq \langle \Delta_3 \rangle$ predicted by OE theory for two randomly mixed populations.²⁴ The aim here is to choose odd A target data with values of Δ_3 not larger than the expected value in order to help insure the data is of reasonable quality, i.e., few missing weak levels. Then the data can be used with some confidence to examine the distribution of reduced neutron widths. Smaller values of Δ_3 tend to reflect data of higher quality. If a small s level is missed or a p -wave level included in an otherwise pure sequence of levels the tendency is for Δ_3 to increase. It should be noted, however, that for two randomly mixed single populations the effect of imperfect data on Δ_3 is less dramatic than the single population case. The normalized reduced widths (total = 331) for the nuclei in Table IV are plotted in Fig. 6. The lack

of agreement between the expected number of small widths, as suggested by the PT distribution, and that found experimentally is striking. Except for ^{197}Au , all the nuclei in Table IV show, with respect to the PT distribution, a lack of weak levels in the first histogram box followed by an excess in the next. The effect is greatest for the ^{151}Sm data. The obvious explanation for the discrepancy is that many weak levels were not detected. However, it is difficult to reconcile the small values of Δ_3 found for these nuclei with so many missed levels. In plotting the data of Fig. 6 it has been assumed that $\langle g\Gamma_n^0 \rangle_+ = \langle g\Gamma_n^0 \rangle_-$, where + and - refer to $I + \frac{1}{2}$ and $I - \frac{1}{2}$, respectively, I being the spin of the target nucleus. If this assumption were incorrect it would not result in an absence of levels in the first histogram box. For example, if $\langle g\Gamma_n^0 \rangle_+$ differed greatly from $\langle g\Gamma_n^0 \rangle_-$ the first few histogram boxes would show an "excess" of levels.

SUMMARY

The results of the Monte Carlo calculations performed here show that for a given amount of a time reversal noninvariant part of Wigner's OE the behavior of the reduced widths is affected much more than the long range correlations between level spacings. Consequently, it seems best to use the OE theory predictions of Δ_3 as a guide to the quality of the data and then use the distribution of the reduced widths to set an upper limit on any time reversal noninvariant part. The high quality even-even target neutron resonance data examined here implies $y < 0.05$ at the 99.7% confidence level. It was found that odd A target reduced width data was in sharp disagreement with the PT distribution even though the Δ_3 values of this data are in excellent agreement with OE theory.

It was also demonstrated that if the matrix elements of Wigner's model are selected from a flat distribution, symmetric about zero, the calculated values of Δ_3 are the same as those found for Gaussian distributed matrix elements. Also, it is noted that the semicircular law gives good fits to the eigenvalue density for matrices intermediate between the OE and UE.

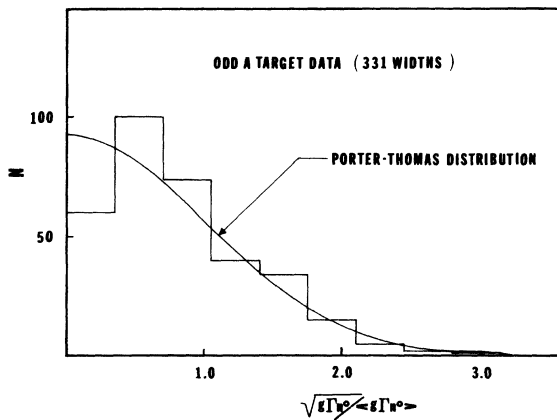


FIG. 6. Distribution of reduced neutron widths for the odd A target nuclei ^{151}Sm , ^{163}Dy , ^{167}Er , ^{175}Lu , ^{177}Hf , and ^{197}Au . The smooth curve is the Porter-Thomas distribution.

- *Work performed under the auspices of the U.S. Energy Research and Development Administration.
- ¹C. E. Porter, *Statistical Theories of Spectra: Fluctuations* (Academic, New York, 1965) contains reprints of papers on the subject up to early 1964. See also M. L. Mehta, *Random Matrices and the Statistical Theory of Energy Levels* (Academic, New York, 1967).
- ²P. B. Kahn and C. E. Porter, Nucl. Phys. 48, 385 (1963).
- ³H. Camarda *et al.*, in *Statistical Properties of Nuclei*, edited by J. B. Garg (Plenum, New York, 1972), p. 205.
- ⁴F. Rahn, H. S. Camarda, G. Hacken, W. W. Havens, Jr., H. I. Liou, J. Rainwater, M. Slagowitz, and S. Wynchank, Phys. Rev. C 6, 251 (1972).
- ⁵F. Rahn, H. S. Camarda, G. Hacken, W. W. Havens, Jr., H. I. Liou, and J. Rainwater, Phys. Rev. C 10, 1904 (1974).
- ⁶H. I. Liou, H. S. Camarda, S. Wynchank, M. Slagowitz, G. Hacken, F. Rahn, and J. Rainwater, Phys. Rev. C 5, 974 (1972).
- ⁷H. I. Liou, H. S. Camarda, G. Hacken, F. Rahn, J. Rainwater, M. Slagowitz, and S. Wynchank, Phys. Rev. C 7, 823 (1973).
- ⁸H. S. Camarda, H. I. Liou, G. Hacken, F. Rahn, W. Makofski, M. Slagowitz, S. Wynchank, and J. Rainwater, Phys. Rev. C 8, 1813 (1973).
- ⁹C. Coceva, Joint Institute for Nuclear Research Report No. JINR-D3-7991, 1975 (unpublished), p. 266-293.
- ¹⁰C. Coceva *et al.*, in *Statistical Properties of Nuclei*, edited by J. B. Garg (Plenum, New York, 1972), p. 447.
- ¹¹W. M. Wilson, E. G. Bilpuch, and G. E. Mitchel, Nucl. Phys. A245, 285 (1975).
- ¹²G. J. Kirouac and H. M. Eiland, Phys. Rev. C 11, 895 (1975).
- ¹³H. I. Liou, G. Hacken, J. Rainwater, and U. N. Singh, Phys. Rev. C 11, 462 (1975).
- ¹⁴H. I. Liou, J. Rainwater, G. Hacken, and U. N. Singh, Phys. Rev. C 11, 1231 (1975).
- ¹⁵H. I. Liou, J. Rainwater, G. Hacken, and U. N. Singh, Phys. Rev. C 11, 2022 (1975).
- ¹⁶R. N. Alves, J. Julien, J. Morgenstern, and C. Samour, Nucl. Phys. A131, 450 (1969).
- ¹⁷N. Rosenzweig, J. E. Monahan, and M. L. Mehta, Nucl. Phys. A109, 437 (1968); L. D. Favro and J. F. MacDonald, Phys. Rev. Lett. 19, 1254 (1967).
- ¹⁸E. P. Wigner, in *Proceedings of the Fourth Canadian Mathematical Congress, Banff, Canada, 1957*, edited by M. S. MacPhail (Univ. of Toronto Press, Toronto, 1959), p. 174.
- ¹⁹E. P. Wigner, Ann. Math. 67, 325 (1958).
- ²⁰A. M. Lane and R. G. Thomas, Rev. Mod. Phys. 30, 257 (1958).
- ²¹C. E. Porter and N. Rosenzweig, Suomalaisen Tredeakat Tormituksia A. VI, No. 44 (1960).
- ²²C. E. Porter and R. G. Thomas, Phys. Rev. 104, 483 (1956).
- ²³For $y \leq 0.1$, $y = \epsilon$, where ϵ is the parameter used by Rosenzweig *et al.* to characterize the strength of the time-reversal violating part of Wigner's model.
- ²⁴F. Dyson and M. L. Mehta, J. Math. Phys. 4, 701 (1963).
- ²⁵F. J. Dyson, J. Math. Phys. 3, 140, 157, 166, 1199 (1962), denoted I, II, III, and T.F.W.
- ²⁶N. Rosenzweig, Phys. Rev. Lett. 1, 24 (1958).
- ²⁷M. Gaudin, Nucl. Phys. 25, 447 (1961).
- ²⁸The $\gamma_{\lambda c}$ values were found by employing Eq. 4 with $S_{jc} = \text{constant}$ and by summing the values of the eigenvector components ($a_{j\lambda}$'s), associated with a given eigenvalue, obtained from the matrix diagonalization.